

Assessment of MODIS and VIIRS Calibration Consistency for Reflective Solar Bands Using Vicarious Approaches

A. Wu^a, Q. Mu^a, A. Angal^a, and X. Xiong^b

^aScience Systems and Applications, Inc., Lanham, MD 20706

^bSciences and Exploration Directorate, NASA/GSFC, Greenbelt, MD 20771

ABSTRACT

The Moderate-Resolution Imaging Spectroradiometer (MODIS) is the key instrument of the NASA's Earth Observing System (EOS) Terra and Aqua missions, launched in December 1999 and May 2002, respectively. The Visible Infrared Imaging Radiometer Suite (VIIRS) expands the MODIS legacy, launched onboard the Suomi National Polar-orbiting Partnership (SNPP) satellite in October 2011 and NOAA20 satellite in November 2017, respectively. The MODIS and VIIRS sensors have a similar design with spectrally matched reflective solar spectral bands (RSB). Their on-board calibration components include a solar diffuser and a solar diffuser stability monitor for RSB, a V-grooved blackbody for the thermal emissive bands (TEB), and a space view as a background reference. This study evaluates the calibration consistency of the Terra and Aqua MODIS RSB based on the current Collection 6.1 L1B data products generated by the NASA MODAPS, which have used consistent calibration coefficient look up tables (LUT) for the entire data-record. In the case of SNPP and NOAA20 VIIRS, the latest L1B data produced by NASA Land SIPS are used. Several independent vicarious approaches are used to examine the stability and consistency of the at-sensor reflectance among MODIS and VIIRS instruments. Vicarious approaches include observations from simultaneous nadir overpasses (SNO), the Libya-4 desert and Dome C snow sites, as well as deep convective clouds (DCC). Impact of existing band spectral difference on the reflectance is corrected using hyperspectral observations provided by Europe Space Agency's SCIAMACHY sensor. Results of this study provide comprehensive assessments of calibration performance, radiometric agreement and associated uncertainties.

Keywords: MODIS, VIIRS, calibration, reflective solar bands, reflectance, vicarious

1. Introduction

The MODIS instrument onboard the Terra and Aqua satellites has been continuously operating for over 20 and 18 years, respectively¹. Both Terra and Aqua are in sun-synchronous, polar orbit with equator crossing time in the morning for Terra and afternoon for Aqua. The swath covers a distance of 2330 km at three nadir spatial resolutions of 0.25, 0.5 and 1.0 km. The 36 spectral bands covering a wavelength range from 0.4 to 2.1 μm are used by the remote sensing and ocean- and land-use communities to retrieve cloud, aerosol, and surface properties²⁻⁵. The MODIS Characterization Support Team (MCST) released the Collection 6.1 (C6.1) Level-1B (L1B)

products, which include the latest calibration algorithm⁶⁻⁷. The MODIS calibration for the reflective solar bands (RSB) relies on the onboard solar diffuser (SD), the SD stability monitor (SDSM), scheduled lunar measurements, and response trends collected over pseudo invariant calibration sites (PICS) located in the North African desert.

VIIRS was developed with a close design heritage to MODIS, currently operating on both SNPP and NOAA20 spacecrafts⁸⁻⁹. VIIRS uses a rotating telescope assembly (RTA) compared to the scan mirror used in MODIS. Major advantages of RTA are better control of stray light, smaller angle of incidence (AOI) range relative to the half angle mirror (HAM), and better protection from contamination and degradation over time. The recently launched (November 18, 2017) NOAA20 is the follow-on mission to the SNPP satellite, launched on October 28, 2011. Both satellites are in the afternoon orbit with a close equator crossing time of 1:30 PM. There are 22 spectral bands with wavelengths ranging from 0.41 to 12.0 μm including 14 RSB, 7 thermal emissive bands, and 1 day-night band (DNB). Each scan covers a 3000 km swath with spatial resolutions of 0.375 km and 0.75 km at nadir for the imaging bands (I-bands) and moderate resolution bands (M-bands), respectively, to provide imagery and radiometric measurements of the land, atmosphere, cryosphere, and oceans¹⁰⁻¹².

The first SNPP and NOAA20 VIIRS imagery were generated a few months after launch after the short-wave/middle-wave infrared (SW/MWIR) and long-wave infrared (LWIR) focal planes were cooled down to their operational temperatures at 80 K. Both sensors went through a series of Intensive Calibration and Validation (ICV) operational activities during the first few months¹³⁻¹⁴. One of the ICV activities designed to support and improve on-orbit calibration of the VIIRS RSB is a series of yaw maneuvers. The SDSM screen transmission derived by combining the yaw maneuver and cumulative on-orbit regular calibration data provided noticeable improvement in the calculation of SD degradation and were used to replace the screen transmission based on prelaunch measurements¹⁵⁻¹⁶. The use of VIIRS lunar observations are based on the similar methodology developed for MODIS. VIIRS Moon and SD views are fixed at the same AOI (60.2°) for the RTA HAM, compared with AOIs of 11.4° (Moon) and 50.2° (SD) for MODIS. The benefit of having two independent sources at the same AOI provides a good opportunity to validate and improve the SD-based calibration results.

The initial goal of this study is to provide an updated assessment of Terra and Aqua MODIS C6.1 RSB calibration consistency using independent vicarious approaches¹⁷⁻¹⁹. Our approaches include the SNO, use of ground targets such as Libya-4 desert and Dome C and deep convective clouds (DCC) to cross-calibrate the instruments²⁰⁻²³. The same approaches were used in our earlier studies to assess the MODIS C6 improvements in comparison with C5. The second goal is to extend the early assessment of the NOAA20 VIIRS to perform a comparison with measurements from SNPP VIIRS, using the latest version 2.0 L1B data produced by NASA Land SIPS (Science Investigator-led Processing Systems). Also included is a comparison between NOAA20 VIIRS and Aqua MODIS for their spectrally matched RSB. One reason that Aqua MODIS is chosen is because it is a better characterized and more stable instrument than Terra MODIS. In addition, the Global Space-based Inter-Calibration System (GSICS), an international organization dedicated to provide

consistent calibration among operational satellite sensors, also uses Aqua MODIS 0.65 μ m band as an absolute calibration reference. Since Aqua MODIS continues to operate nearly a decade beyond its design life, the transfer of the calibration reference from Aqua-MODIS to SNPP or NOAA20 VIIRS is necessary to ensure a consistent retrieval product across these sensors.

2. Vicarious approaches

Various vicarious approaches are used to examine the calibration consistency between Terra and Aqua MODIS, NOAA-20 and S-NPP VIIRS and between Aqua MODIS and S-NPP VIIRS for the spectrally matched bands ²⁰⁻²³. The primary approach is the use of simultaneous nadir overpasses (SNO) ²⁴. This approach is based on a direct pixel level comparison between the two crossover sensors. Since there is no simultaneous crossover between Terra and Aqua or S-NPP and NOAA-20 satellites, a third sensor is used as a transfer radiometer. Since SNOs occur periodically between MODIS and VIIRS, either one can be used as a transfer radiometer. A double difference method is used to compare two MODIS or VIIRS sensors. There is an abundance of VIIRS and MODIS SNOs, with nearly one SNO event every three days. The frequent location of these SNOs is in the high-latitude region. The SNO data sets collected in this study are all from the MODIS and VIIRS crossovers with less than 30 seconds. An averaged ratio of reflectance between VIIRS and MODIS is determined once a statistically sufficient sample size is obtained from each SNO with a restriction of a 10.0° off nadir range. Since there is no restriction of SNO on location and surface type, results of this approach contain data from a wide variety of scene types. Figure 1 shows an example of pixel-to-pixel comparison of reflectance between Aqua MODIS and SNPP VIIRS at the 0.65 and 0.85 μ m bands based on a SNO event from Oct. 8, 2019. Similarly, Aqua MODIS can be used as a transfer radiometer to make comparison of NOAA-20 and S-NPP VIIRS.

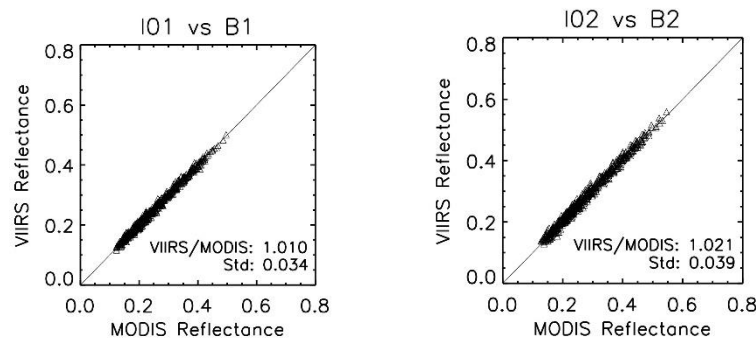


Figure 1. Comparison of SNPP VIIRS I1 and I2 and Aqua bands 1 and 2 for pixel by pixel matched reflectances.

The second approach is based on reflectances collected over PICS located in the Libyan Desert including the widely used Libya-4 desert site (28.5°N, 23.4°E) and the Dome C ice/snow site on

the Antarctic Plateau^{20-21, 25}. The main reason that these PICS are used is because of the relatively high and nearly constant reflectance with little vegetation. Similar to the SNO approach, we choose near-nadir overpasses with view zenith angles less than 5.0° over the site, obtained from 16-day repeatable orbits. Since the view and solar zenith angles of the VIIRS and MODIS observations over the site can be selected to have a similar angular range, a site-dependent bi-directional reflectance function (BRDF) model based on measurements from one sensor (either VIIRS or MODIS) can be applied to measurements from another sensor for their spectrally matched bands. The BRDF model's coefficients are derived from cumulative data typically for a three-year period to cover the seasonal cycle of the angular parameters.

The use of DCCs is another method and particularly useful for the short-wave infrared (SWIR) bands in assessing their long-term calibration stability²²⁻²³. DCCs are the coldest natural earth targets in the tropics and can be easily identified using a brightness temperature (BT) threshold in the atmospheric IR window. The advantage of the DCC technique is that DCCs are at the tropopause level, where the effects of atmospheric absorption are significantly reduced. In addition, they are extremely bright earth targets with a nearly Lambertian reflectance. Unlike any PICS site, a DCC mode value is used, which is obtained using a histogram of reflectances collected every month. In addition, a DCC BRDF model is normally used to remove its seasonal variations.

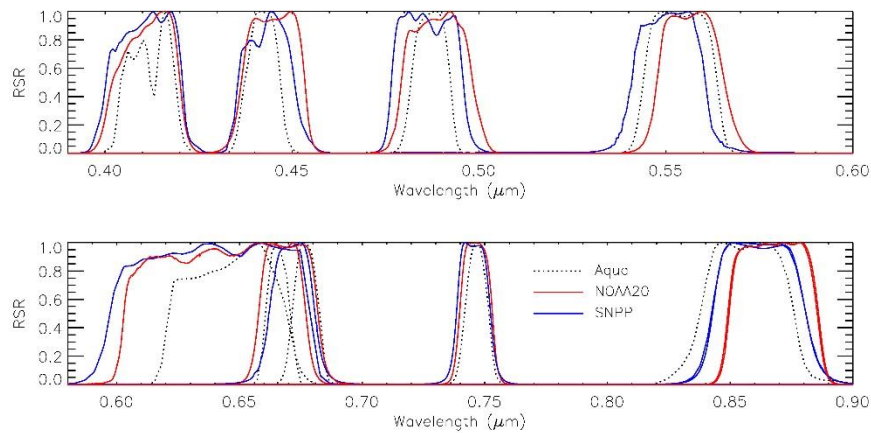


Figure 2. RSR for spectrally match bands in the visible and near-infrared region from Aqua MODIS, SNPP and NOAA20.

There are existing differences in the relative spectral response (RSR) among MODIS, SNPP and NOAA20 VIIRS (Figure 2). The RSR induced differences are estimated using SCIAMACHY observations, one of ten instruments aboard of ESA's Environmental Satellite, ENVISAT. It has a relatively high spectral resolution (0.2 nm to 0.5 nm) and a wide wavelength range (240 nm to 1700 nm). Although the ENVISAT mission ended on May 9, 2012, it provides a decade-long global dataset from August 2002 to April 2012. The SCIAMACHY data collected in 2004 is used, based on the Level-1B data product (SCI_NL_1P, version 7.03). Information on the viewing scene identification is based on Terra MODIS co-location data and the corrections are calculated using

averaged SCIAMACHY overpasses for the various surfaces including land and cloud. The calculation for the SNO surfaces is based on an averaged SCIAMACHY profile using overpasses over multiple scene types, since data are collected from varying scene-types. For DCC surfaces, the RSR correction values are taken from the SCIAMACHY-based spectral band adjustment factor (SBAF) tool provided by NASA-LaRC (<https://clouddsgate2.larc.nasa.gov/cgi-bin/site/showdoc?mnemonic=SBAF>)²⁶. Figure 3 shows the RSR correction for reflectance ratios between NOAA-20 and SNPP VIIRS for the four surfaces. The correction is expressed as a ratio of NOAA-20 to SNPP reflectance ratio determined using the SCIAMACHY observations for the four surfaces. A large variation for M4 among the surfaces is mainly due to the existing central wavelength shift between SNPP and NOAA-20. Figure 4 shows the RSR correction between NOAA-20 VIIRS and Aqua MODIS spectrally match RSB for the three surfaces. The reason that M5 has a significantly large correction is due to the existing spectral wavelength shift between VIIRS M5 and MODIS band 1. Results of the RSR correction for the DCC surface is not included here because most of Aqua MODIS bands considered here saturate while viewing the DCC.

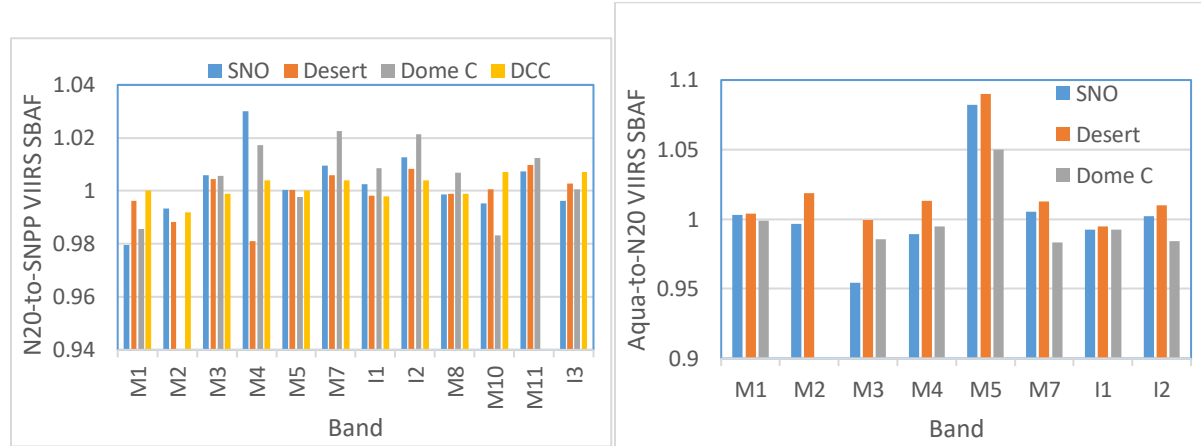


Figure 3. SBAF between NOAA20 and SNPP RSB for SNO, desert, Dome C and DCC.

Figure 4. SBAF between Aqua and NOAA20 RSB for SNO, desert, Dome C.

3. Terra and Aqua MODIS calibration consistency

For the SNO approach, the calibration consistency between Terra and Aqua is estimated since 2012 when SNPP VIIRS became operational. Using SNPP as a transfer, the trends of Terra and Aqua MODIS to VIIRS reflectance SNO ratio are shown for band 1 in Figure 5. Data gaps in the Terra MODIS trend are due to exclusion of periods when Terra and SNPP SNOs are at solar zenith angles greater than 80.0°. There are seasonal variations in the trends likely due to remaining BRDF effect. On average, Terra MODIS band 1 reflectance is 1.15% lower than Aqua. Since the RSB of the two sensors have almost identical relative spectral response, no correction for the spectral

differences is applied. For the PICS approaches, the Terra reflectances normalized by the site dependent BRDF derived from Aqua observations are averaged over mission to estimate their calibration consistency. For the DCC approach, instead of a sensor dependent BRDF, mode values obtained from the histogram of reflectances collected each month are used to compare between the two sensors. Table 1 shows the differences of Terra MODIS relative to Aqua MODIS determined using the four vicarious approaches. The SNO approach has a relatively short data period compared with other approaches covering the time period from 2012 to present. For visible (VIS) and near-IR (NIR) bands, the relative differences are within 1.5% from all four approaches. A slightly larger difference is observed for bands 3 and 15 in the SNO method. For band 3, it is likely due to the significant spectral mismatch between MODIS and VIIRS. Therefore, the result has a relatively large uncertainty, compared with other VIS/NIR bands. For band 15, a high-gain ocean band, available SNO points are limited due to saturation while observing surfaces other than clear ocean. For the SWIR bands, results from the DCC and desert approach are more reliable, as their uncertainties are much lower than the other two approaches. One possible reason for the large uncertainties in the SNO and Dome C approaches is due to their high sensitivity to clouds. Although DCC results generally have lower uncertainties than other approaches for the SWIR bands, there is concern about its high sensitivity to the BT threshold used to identify DCC pixels. Since the BT threshold is set at around a very low temperature of 205K, errors in BT due to calibration are magnified at extreme low temperatures, which could affect the derived DCC mode reflectances for the SWIR bands. In addition, Terra SWIR bands show greater electronic crosstalk impact than Aqua due to contamination from a few thermal emissive bands. Given these uncertainties for the SWIR bands, the relative differences between Terra and Aqua are within 2% but with a high uncertainty of 2 to 4% depending on approach.

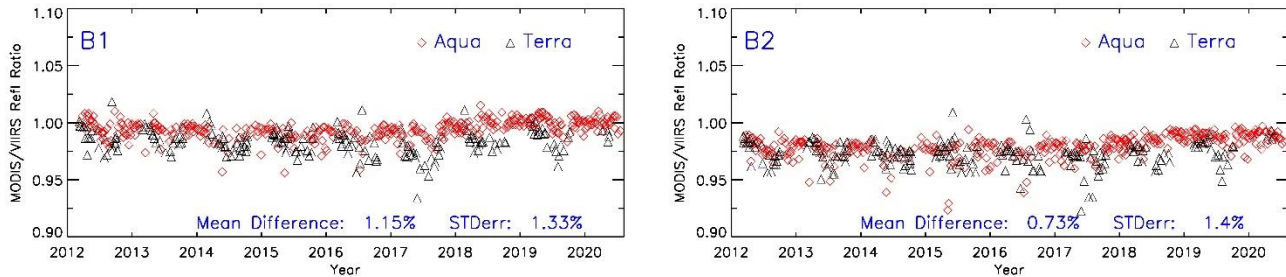


Figure 5. Comparison of Terra and Aqua MODIS reflectances for bands 1 and 2 obtained from SNO with SNPP VIIRS.

Table 1. Terra and Aqua MODIS RSB comparison. Results are provided in percentage difference (Terra – Aqua) (%). Numbers within the bracket are standard errors. Those marked “n/a” are either not applicable or excluded due to saturation.

Band (um)	VIS/NIR										SWIR		
	B1 0.65	B2 0.86	B3 0.47	B4 0.55	B8 0.41	B9 0.44	B10 0.49	B12 0.55	B13 L 0.67	B15 0.75	B5 1.24	B6 1.64	B7 2.13
SNO	-1.2 (1.3)	-0.8 (1.4)	2.3 (4.2)	-0.8 (1.1)	0.5 (1.6)	1.0 (1.7)	-0.2 (2.2)	-1.3 (3.2)	-1.2 (3.1)	-2.9 (5.3)	4.0 (3.2)	2.0 (4.8)	n/a
Desert	-1.2 (1.0)	0.3 (1.1)	0.8 (1.7)	-0.3 (1.2)	-0.2 (1.9)	-0.5 (1.7)	n/a	n/a	n/a	n/a	1.8 (1.3)	0.2 (1.1)	2.1 (2.3)
Dome C	-0.8 (2.6)	0.6 (2.6)	0.8 (1.7)	-0.1 (2.7)	n/a	n/a	n/a	n/a	n/a	n/a	5.6 (6.9)	n/a	n/a
DCC	0.2 (1.5)	n/a	1.8 (1.7)	0.8 (1.5)	n/a	n/a	n/a	n/a	n/a	n/a	1.1 (1.3)	-0.4 (2.1)	-3.1 (2.9)

4. SNPP and NOAA20 VIIRS calibration consistency

Trends of near-nadir reflectance obtained from the four vicarious approaches as shown in Figures 6 to 9 indicate that SNPP and NOAA20 VIIRS RSB are stable, although the data collection period for NOAA20 is less than three years. For the desert and Dome C approaches, a site-dependent BRDF model derived using SNPP VIIRS reflectance data is applied to NOAA20 VIIRS. Results indicate NOAA20 reflectances are systematically lower than SNPP by 1 to 4% for most RSB, except the shortest wavelength bands M1, M2 and M3. Some of the observed differences are due to existing RSR differences (Figure 2), which also change with the surface type and atmospheric conditions.

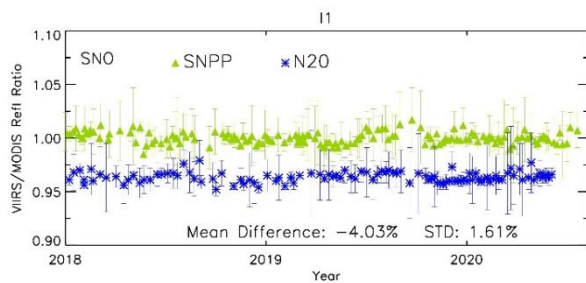


Figure 6. Comparison of SNPP and NOAA20 VIIRS I1 reflectance from SNO with Aqua MODIS

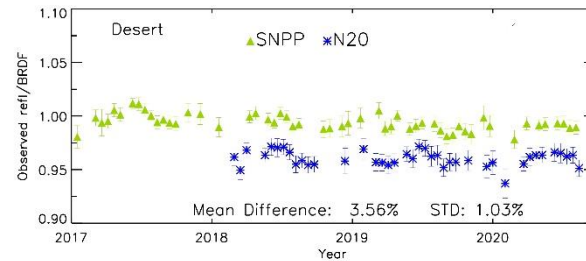


Figure 7. Comparison of SNPP and NOAA20 VIIRS I1 reflectance for the Libya-4 desert site

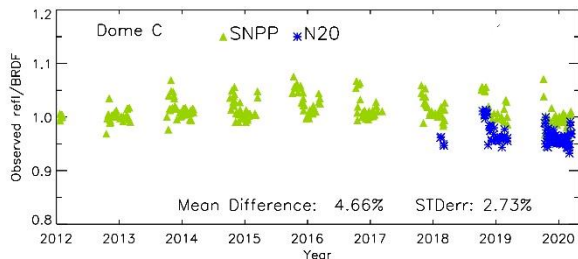


Figure 8. Comparison of SNPP and NOAA20 VIIRS I1 reflectance for the Dome C site.

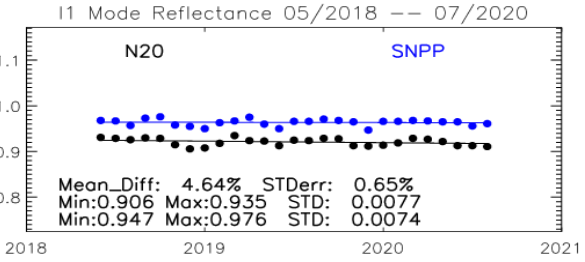


Figure 9. Comparison of SNPP and NOAA20 VIIRS I1 reflectance for DCC.

The reflectance differences after the RSR correction are shown in Table 2. In general, the differences are more consistent among the four surfaces after the RSR correction, particularly for M4. The shortest wavelength bands M1 to M3 show the largest differences ranging from 4 to 6%, compared to differences between 2 and 4% for other longer wavelength bands. One reason for the increased differences in M1 to M3 in the NASA SIPS Collection-2 L1B product is due to a calibration offset adjustment of up to 2% compared with other bands. For the DCC approach, results for M1 and M4 are particularly different from those produced by the other three approaches. For these two bands, the DCC SBAF values are relatively closer to the SNO SBAF values, indicating that errors in the RSR correction do not completely explain the large observed differences. For the SWIR bands, similar to the case between Terra and Aqua MODIS, there are large uncertainties in the SNO and Dome C approaches possibly due to their high sensitivity to clouds. Our recent result showed that reflectances from N20 VIIRS RSB are lower than those from SNPP by 4% on average and more negative biases occur in the shortest wavelength bands M1 to M3²¹. Similar results of the radiometric biases between the two instruments were also observed in other recent studies based on L1B product generated by NOAA interface data processing segment (IDPS)²⁷⁻²⁸. Note there are some noticeable differences depending on wavelength between NASA SIPS and NOAA IDPS for SNPP VIIRS L1B reflectance products due to differences in calibration strategies. As discussed in our earlier studies, analysis of instrument prelaunch SD data can provide more information.

Table 2. SNPP and NOAA20 VIIRS RSB comparison. Results are provided in percentage difference (SNPP – NOAA20) (%). Numbers within the bracket are standard errors. Those marked “n/a” are either not applicable or excluded due to saturation.

Band (um)	VIS/NIR										SWIR		
	M1 0.65	M2 0.86	M3 0.47	M4 0.55	M5 0.41	M7 0.44	I1 0.49	I2 0.55	M8 0.67	M9 0.75	M10 1.24	M11 1.64	I3 2.13
SNO	6.3 (1.8)	5.2 (1.6)	4.9 (1.8)	3.4 (1.6)	4.7 (2.3)	3.5 (1.8)	3.8 (1.6)	3.6 (1.8)	3.3 (1.3)	5.9 (6.0)	3.0 (3.1)	4.1 (9.1)	4.7 (3.2)

Desert	7.0 (1.3)	6.1 (1.2)	4.3 (1.2)	3.7 (1.2)	5.1 (0.9)	2.8 (0.9)	3.7 (1.1)	3.1 (1.1)	2.2 (1.3)	n/a	1.5 (0.9)	0.8 (2.2)	4.7 (1.0)
Dome C	6.7 (1.4)	n/a	4.7 (1.4)	5.2 (2.9)	5.5 (2.8)	2.9 (2.9)	3.8 (2.7)	3.3 (3.0)	2.6 n/a	n/a	5.2 n/a	3.1 n/a	3.5 n/a
DCC	1.0 (1.5)	6.4 (1.6)	6.0 (1.6)	9.1 (1.6)	3.1 (1.6)	3.7 (1.5)	6.1 (1.6)	5.9 (1.6)	2.2 (0.9)	1.0 (2.1)	2.1 (2.5)	2.4 (1.9)	4.9 (2.6)

5. NOAA20 VIIRS and Aqua MODIS calibration consistency

Comparison is also performed between NOAA20 VIIRS and Aqua MODIS for their spectrally matched RSB. The DCC results for bands not impacted by saturation are also included. As discussed earlier, errors in the BT threshold due to calibration differences between VIIRS and MODIS sensors are expected to add uncertainty in this comparison. Also, the DCC approach is more sensitive to the BT threshold for the SWIR bands. The NOAA20 VIIRS and Aqua MODIS reflectance differences after the RSR correction are shown in Table 3. Results indicates that NOAA20 is consistently lower than Aqua by about 1.0 to 3.0% and the shortest wavelength bands M1 and M2 have additional large biases up to 5%. In general, the differences are smaller than those between NOAA20 and SNPP as shown in Table 2. Results also show that differences among the three approaches are up to 2.0%, indicating there are still large uncertainties in the methodologies. It is expected that errors due to existing residual BRDF impact on the comparison data is about 1%, plus additional 0.5% due to unavailability of a scene-specific real-time RSR correction.

Table 3. NOAA-20 and Aqua MODIS RSB comparison. Results are provided in percentage difference (NOAA20 – Aqua) and standard error (%).

		RSB (%)					
Method	Period	M1/B8	M2/B9	M4/B4	M7/B2	I1/B1	I2/B2
SNO	2018-2019	-2.3 ± 1.6	-3.4 ± 1.5	-2.3 ± 1.5	-3.1 ± 1.7	-2.8 ± 1.5	-3.1 ± 1.7
Desert	2018-2019	-4.2 ± 1.1	-5.3 ± 0.8	-2.4 ± 0.8	-0.6 ± 0.5	-3.6 ± 0.7	-0.9 ± 0.8
Dome C	2018-2019	-3.9 ± 1.0	n/a	-2.6 ± 1.8	-1.0 ± 2.2	-2.9 ± 1.8	-1.3 ± 2.2
DCC	2018-2020	n/a	n/a	-2.8 (1.5)	n/a	-5.3 (1.5)	n/a

6. SUMMARY

This study provides an updated assessment of the calibration stability among Terra and Aqua MODIS, SNPP and NOAA20 VIIRS RSB. For MODIS, C6.1 L1B product is used and for VIIRS,

the version-2 L1B product generated by NASA SIPS via a recent reprocessing over the entire mission is used. Different vicarious approaches (SNO, desert, Dome C and DCC) are used to compare their at-sensor reflectances after correction for band spectral differences. Between Terra and Aqua MODIS, the relative differences are within 2% for all RSB except for the SWIR bands where a high uncertainty of 2 to 4% is observed depending on approach. In the case of SNPP and NOAA20 VIIRS RSB, comparison shows that the reflectances of the shortest wavelength bands M1 to M3 of NOAA20 are lower than SNPP by about 4 to 7%. At longer wavelengths, the biases are between 2 and 4%. A further comparison between NOAA20 and Aqua MODIS indicates that NOAA20 is consistently lower than Aqua by about 1.0 to 3.0% and a few shortest wavelength bands show the largest differences. Results also show that differences among the four approaches are up to 2.0%, indicating there are still large uncertainties that need to be considered. The results of this study produce useful information about potential impacts on the comparison of downstream science products. It also provides findings that are useful for diagnosing and improving future calibration algorithms.

References

1. Salomonson, V. V., Barnes, W. L., Maymon, P. W., Montgomery, H. E., and Ostrow, H.: MODIS: Advanced facility instrument for studies of the Earth as a system, IEEE T. Geosci. Remote, 27, 145–153, (1989).
2. Esaias, E.; Abbott, M.; Barton, I.; Brown, O.; Campbell, J.; Carder, K.; Clark, D.; Evans, R.; Hoge, F.; Gordon, H.; Balch, W.; Letelier, R.; Minnett, P. An Overview of MODIS Capabilities for Ocean Science Observations. IEEE Trans. Geosci. Remote Sensing, 36, 1250-1265, (1998).
3. Levy, R. C., Remer, L. A., and Dubovik, O.: Global aerosol optical properties and application to Moderate Resolution Imaging, Spectroradiometer aerosol retrieval over land, J. Geophys. Res. Atmos., 112, D13210, doi:10.1029/2006JD007815, (2007).
4. Justice, C.; Vermote, E.; Townshend, J.; Defries, R.; Roy, D.; Hall, D.; Salomonson, V.; Privette, J.; Riggs, G.; Strahler, A.; Lucht, W.; Myneni, R.; Lewis, P.; Barnsley, M. The Moderate Resolution Imaging Spectroradiometer (MODIS): Land Remote Sensing for Global Change Research. IEEE Trans. Geosci. Remote Sensing, 36, 1228-1249, (1998).
5. King, M.; Menzel, P.; Kaufman, Y.; Tanre, D.; Gao, B.; Platnick, S.; Ackerman, S.; Remer, L.; Pincus, R.; Hubanks, P. Cloud and Aerosol Properties, Precipitable Water, and Profiles of Temperature and Water Vapor from MODIS. IEEE Trans. Geosci. Remote Sensing, 41, 442-458, (2003).
6. Xiong, X.; Chiang, K.; Esposito, J.; Guenther, B.; Barnes, W.L. "MODIS On-orbit Calibration and Characterization," Metrologia, 40, 89-92, (2003).
7. Xiong, X., A. Angal, K. Twedt, H. Chen, D. Link, X. Geng, E. Aldoretta, Q. Mu, "MODIS Reflective Solar Bands On-Orbit Calibration and Performance," IEEE TGRS, vol 57, issue 9, pp 6355-6371, (2019).
8. Schueler, C. F., E. Clement, P. Ardanuy, C. Welsh, F. De Luccia, and H. Swenson, NPOESS VIIRS sensor design overview," Proc. SPIE, 4483, 11–23, (2002).

9. Murphy, R.P., P. E. Ardanuy, F. De Luccia, J. E. Clement, and C. Schueler, "The visible infrared imaging radiometer suite," in Earth Science Satellite Remote Sensing, vol. 1, New York, USA: Springer-Verlag, pp. 199–223, (2006).
10. Justice, C. O., M. O. Román, I. Csizar, E. F. Vermote, 570 R. E. Wolfe, S. J. Hook, M. Friedl, Z. Wang, C. B. Schaaf, T. Miura, M. Tschudi, G. Riggs, D. K. Hall, A. I., Lyapustin, S. Devadiga, C. Davidson, and E. J. Masuoka, "Land and cryosphere products from Suomi NPP VIIRS: Overview and status," *Journal of Geophysical Research (Atmospheres)*, 118, 9753–9765, doi:10.1002/jgrd.50771, (2013).
11. Wang, M., X. Liu, L. Tan, L. Jiang, S. Son, W. Shi, K. Rausch, and K. Voss, "Impacts of VIIRS SDR performance on ocean color products," *Journal of Geophysical Research (Atmospheres)*, 118, 10,347, doi:10.1002/jgrd.50793, (2013).
12. Liu, H., L. A. Remer, J. Huang, H.-C. Huang, S. Kondragunta, I. Laszlo, M. Oo, and J. M. Jackson, Preliminary evaluation of S-NPP VIIRS aerosol optical thickness, *Journal of Geophysical Research (Atmospheres)*, 119, 3942–3962, (2014).
13. Cao, C., F. Deluccia, X. Xiong, R. Wolfe, and F. Weng, "Early On-Orbit Performance of the Visible Infrared Imaging Radiometer Suite Onboard the Suomi National Polar-Orbiting Partnership (S-NPP) Satellite," *IEEE TGRS* , vol.52, no.2, 1142-1156, (2014).
14. Xiong, X., J. Butler, K. Chiang, B. Efremova, J. Fulbright, N. Lei, J. McIntire, H. Oudrari, J. Sun, Z. Wang, A. Wu, "VIIRS on-orbit calibration methodologies and performance," *Journal of Geophysical Research*, Volume 119, Issue 9, pp 5065-5078, DOI: 10.1002/2013JD020423, (2014).
15. Lei, N.; Xiong, X.; Products of the SNPP VIIRS SD Screen Transmittance and the SD BRDFs from Both Yaw Maneuver and Regular On-orbit Data. *IEEE Trans. Geosci. Remote Sens.*, 55, 4, 1975-1987, (2017).
16. Lei, N., and X. Xiong, "Determination of the NOAA-20 VIIRS screen transmittance functions with both the yaw maneuver and regular on-orbit calibration data", *Applied Optics*, vol 59, issue 10, pp. 2992-3001, (2020).
17. Abdou, B.A., C.J. Bruegge, M.C. Helmlinger, J.E. Conel, S.H. Pilorz, W. Ledeboer, B.J. Gaitley, K.J. Thome, Vicarious calibration experiment in support of the Multi-angle Imaging SpectroRadiometer, *IEEE Transactions on Geoscience and Remote Sensing*, Vol: 40, Issue: 7 , pp. 1500-1511, DOI: 10.1109/TGRS.2002.801582, (2002).
18. Biggar, S.F., K.J. Thome, W. Wisniewski, Vicarious radiometric calibration of EO-1 sensors by reference to high-reflectance ground targets, *IEEE Transactions on Geoscience and Remote Sensing*, Vol: 41 , Issue: 6 , pp. 1174-1179, DOI: 10.1109/TGRS.2003.813211, (2003).
19. Doelling, D.R., D. Morstad, B.R. Scarino, R. Bhatt, A. Gopalan, The Characterization of Deep Convective Clouds as an Invariant Calibration Target and as a Visible Calibration Technique, *IEEE Transactions on Geoscience and Remote Sensing*, vol. 51, 3, 1147 – 1159, DOI: 10.1109/TGRS.2012.2225066, (2012).
20. Wu, A., X. Xiong, D.R. Doelling, D. Morstad, A. Angal, R. Bhatt, Characterization of Terra and Aqua MODIS VIS, NIR, and SWIR Spectral Bands' Calibration Stability. *IEEE Transactions on Geoscience and Remote Sensing*, 51, 7, pp. 4330-4338, (2012).
21. Wu, A., K. Chiang, N. Lei, X. Xiong, Evaluation of NOAA-20 VIIRS reflective solar bands calibration performance using vicarious approaches, *Proceedings Volume 11151, Sensors, Systems, and Next-Generation Satellites XXIII; 1115125*, DOI: 10.1117/12.2532573, (2019),
22. Doelling, D. R., A. Wu, X. Xiong, B.R. Scarino, R. Bhatt, C. O. Haney, D. Morstad, A. Gopalan, The Radiometric Stability and Scaling of Collection 6 Terra- and Aqua-MODIS VIS, NIR, and

- SWIR Spectral Bands, IEEE Transactions on Geoscience and Remote Sensing, Vol. 53 , Issue: 8 , pp. 4520 – 4535, 2015.
- 23. Mu, Q., A. Wu, X. Xiong, D. R. Doelling, A. Angal, T. Chang, and R. Bhatt, Optimization of a Deep Convective Cloud Technique in Evaluating the Long-Term Radiometric Stability of MODIS Reflective Solar Bands, *Remote Sensing*, vol. 9 (6), issue 535, (2017).
 - 24. Cao, C., M. Weinreb, H. Xu, Predicting simultaneous nadir overpasses among polar-orbiting meteorological satellites for intersatellite calibration of radiometers. *Journal of Atmospheric and Oceanic Technology*, 21, pp. 537-542, 2004.
 - 25. Uprety, S.; C. Cao.; Suomi NPP VIIRS Reflective Solar Band On-Orbit Radiometric Stability and Accuracy Assessment Using Desert and Antarctica Dome C Sites. *Remote Sensing of Environment*, 166,106–115, (2015).
 - 26. Scarino, B.R., D.R. Doelling, P. Minnis, A. Gopalan, T. Chee, R. Bhatt, C. Lukashin, C. Haney, A Web-Based Tool for Calculating Spectral Band Difference Adjustment Factors Derived From SCIAMACHY Hyperspectral Data, *IEEE Transactions on Geoscience and Remote Sensing*, vol. 54, no. 5, pp. 2529 – 2542, (2016).
 - 27. Uprety, S., C. Cao, X. Shao, Radiometric consistency between GOES-16 ABI and VIIRS on Suomi NPP and NOAA-20, *J. Appl. Remote Sens.* 14(3), 032407, doi: 10.1117/1.JRS.14.032407 (2020).
 - 28. Uprety, S., C. Cao, S. Blonski, X. Shao, Evaluating NOAA-20 and S-NPP VIIRS radiometric consistency, Proc. SPIE 10781, Earth Observing Missions and Sensors: Development, Implementation, and Characterization V, 107810V <https://doi.org/10.1117/12.2324464>, (2018).